

This is the accepted manuscript made available via CHORUS. The article has been published as:

Thermally Mediated Mechanism to Enhance Magnetoelectric Coupling in Multiferroics

C.-M. Chang, B. K. Mani, S. Lisenkov, and I. Ponomareva

Phys. Rev. Lett. **114**, 177205 — Published 1 May 2015

DOI: [10.1103/PhysRevLett.114.177205](https://doi.org/10.1103/PhysRevLett.114.177205)

An unusual route to enhanced magnetoelectric coupling in multiferroics

C.-M. Chang,¹ B. K. Mani,¹ S. Lisenkov,¹ and I. Ponomareva¹

¹*Department of Physics, University of South Florida, Tampa, Florida 33620, USA*

Abstract

The main road block on the way to practical realization of magnetoelectric devices is the lack of multiferroics with strong magnetoelectric coupling. We propose an unusual route to dramatically enhance this coupling through thermally mediated mechanism. Such thermally mediated magnetoelectric effect is quantified by an isentropic rather than isothermal magnetoelectric response and is computed here from first-principles. A robust enhancement of the magnetoelectric coupling is predicted for both naturally occurring and heterostructured materials.

Magnetoelectric multiferroics are the materials that exhibit both electric and magnetic orderings at the same time. They have attracted an unprecedented attention in the recent years owing to their potential to exhibit magnetoelectric coupling [1–7]. Such coupling could open the ways to innovative applications such as four-state logic in a single device, magnetoelectric random access memories, electrically controlled exchange bias applications [8]. Most of these applications, however, require strong coupling between electric and magnetic degrees of freedom. As a result the search was directed toward discovery of multiferroics with enhanced magnetoelectric coupling. While such a search resulted in a plethora of scientific breakthroughs [7, 9, 10], the discovery of multiferroics with technologically significant magnetoelectric coupling eluded researchers. Once again we are forced to appreciate the importance of the fundamental science that “contra-indicates” ferroelectricity and ferromagnetism [11]. At the same time, one may begin to wonder if we could “trick” the nature into enhancing the magnetoelectric coupling through indirect mechanisms. One example is the strain-mediated magnetoelectric coupling in heterostructures made of ferroelectric and ferromagnetic materials [12]. Indeed such materials exhibit the largest values of magnetoelectric coupling to date [13]. At the same time, such mechanism relies on an excellent lattice match between rather dissimilar materials which could be challenging to achieve in practice. In this paper we propose an unusual route to a robust enhancement of magnetoelectric coupling via thermally mediated mechanism. Such mechanism offers the advantages of universality as it applies to both intrinsic (naturally occurring) and extrinsic (heterostructured) multiferroics; and of flexibility in coupling engineering.

The linear magnetoelectric coupling is usually defined as a tensor with components $\delta_{\alpha\beta} = \frac{\partial M_\alpha}{\partial E_\beta}$, where M_α and E_β are the α th component of the magnetization and β th component of the electric field, respectively [14]. Alternatively it could be defined as $\delta_{\alpha\beta} = \frac{\partial P_\alpha}{\partial B_\beta}$, where P and B are the polarization and the magnetic induction, respectively. It is often implicitly assumed that the derivatives are taken under constant temperature, making $\delta_{\alpha\beta}$ an isothermal coupling. To achieve temperature mediated magnetoelectric coupling we allow the temperature, T , to vary. Using temperature, electric, and magnetic fields as independent thermodynamical variables, while entropy, polarization and magnetization as their dependent counterparts, we write the infinitesimal change in magnetization as $dM_\alpha = \left(\frac{\partial M_\alpha}{\partial T}\right)_{EB} dT + \left(\frac{\partial M_\alpha}{\partial E_\beta}\right)_{TB} dE_\beta + \left(\frac{\partial M_\alpha}{\partial B_\gamma}\right)_{TE} dB_\gamma$. Let us now apply an electric field slowly and under adiabatic conditions to ensure that the total entropy, S , is conserved. The

associated linear isentropic magnetoelectric effect is

$$\left(\frac{\partial M_\alpha}{\partial E_\beta}\right)_{SB} = \left(\frac{\partial M_\alpha}{\partial T}\right)_{EB} \left(\frac{\partial T}{\partial E_\beta}\right)_{SB} + \left(\frac{\partial M_\alpha}{\partial E_\beta}\right)_{TB}. \quad (1)$$

Here the last term is the usual isothermal linear magnetoelectric coupling. Note, that for the remainder of the paper we will implicitly assume that all the couplings are linear unless otherwise stated. From Eq.(1) we observe that the difference between the isentropic and isothermal magnetoelectric coupling is proportional to the pyromagnetic coefficient, $\left(\frac{\partial M}{\partial T}\right)_{EB}$, and the electrocaloric effect, $\left(\frac{\partial T}{\partial E}\right)_{SB}$. First of all, we notice that the equation predicts that the isentropic magnetoelectric coupling can occur even in materials with a negligible isothermal one. Indeed, unlike its isothermal counterpart, the isentropic coupling is temperature mediated and therefore does not require strong intrinsic coupling between magnetic and electric order parameters. Here we recall that the small values of magnetoelectric coupling remains the main road block on the way to practical applications of magnetoelectric multiferroics. Secondly, thanks to its temperature mediated nature, the isentropic coupling can be enhanced or otherwise engineered in a variety of ways. For example, typically both pyromagnetic and electrocaloric effects in multiferroics are maximized around transition temperatures. So the isentropic magnetoelectric effect can be manipulated by tuning transition temperatures through nanostructuring, strain engineering and others. Another possible way to enhance the effect is through heterostructuring materials with good pyromagnetic and electrocaloric properties. Interestingly, heterostructuring has proven to be a potent way to enhance the isothermal magnetoelectric coupling through strain-mediated mechanism [13]. At the same time, strain-mediated mechanism relies on good lattice match which may be challenging to achieve. The isentropic coupling, on the other hand, does not have such a requirement as it relies on thermal equilibrium between the components of the heterostructure.

In materials with nonvanishing isothermal magnetoelectric coupling the isentropic coupling could be further enhanced provided that both terms on the right hand side of Eq.(1) are of the same sign. This requirement could always be met in a polar phase of ferroelectrics where the sign of $\left(\frac{\partial T}{\partial E}\right)_{SB}$ is controlled by the direction of the electric field [15]. By analyzing Eq.(1) we find that the isentropic magnetoelectric coupling exceeds its isothermal counterpart if $\left(\frac{\partial M_\alpha}{\partial T}\right)_{EB} \left(\frac{\partial T}{\partial E_\beta}\right)_{TB} > -2 \left(\frac{\partial M_\alpha}{\partial E_\beta}\right)_{TB}$.

Next we explore the isentropic electromagnetic effect $\left(\frac{\partial P_\alpha}{\partial B_\beta}\right)_{SE}$. Note that unlike the case

of an isothermal coupling for the isentropic one $\left(\frac{\partial P_\alpha}{\partial B_\beta}\right)_{SE} \neq \left(\frac{\partial M_\alpha}{\partial E_\beta}\right)_{SB}$. Here we start with $dP_\alpha = \left(\frac{\partial P_\alpha}{\partial T}\right)_{EB} dT + \left(\frac{\partial P_\alpha}{\partial E_\gamma}\right)_{TB} dE_\gamma + \left(\frac{\partial P_\alpha}{\partial B_\beta}\right)_{TE} dB_\beta$, where P is the electric polarization. A slow application of magnetic induction under adiabatic condition will result in an isentropic electromagnetic coupling

$$\left(\frac{\partial P_\alpha}{\partial B_\beta}\right)_{SE} = \left(\frac{\partial P_\alpha}{\partial T}\right)_{EB} \left(\frac{\partial T}{\partial B_\beta}\right)_{SE} + \left(\frac{\partial P_\alpha}{\partial B_\beta}\right)_{TE}. \quad (2)$$

The latter relationship is symmetric to Eq.(1) if we interchange polarization with magnetization and the electric field with the magnetic induction. This symmetry suggests that the previous analysis is also valid for the isentropic electromagnetic coupling if the proper fields interchange is applied.

To demonstrate the aforementioned enhancement of magnetoelectric and electromagnetic couplings under adiabatic conditions we turn to the room temperature magnetoelectric multiferroic BiFeO₃. BiFeO₃ is an antiferromagnet. Therefore, instead of looking for coupling between the magnetization and electric field we will look into the coupling between the antiferromagnetic vector and the electric field. Such coupling is important for the electrically controlled exchange bias [3]. It can be derived similarly to Eq.(1) where the magnetization is replaced with the antiferromagnetic vector, \mathbf{A} . Our approach is to use first-principles-based simulations to compute $\left(\frac{\partial A_\alpha}{\partial T}\right)_{EB}$, $\left(\frac{\partial T}{\partial E_\beta}\right)_{SB}$, $\left(\frac{\partial A_\alpha}{\partial E_\beta}\right)_{TB}$, and $\left(\frac{\partial P_\alpha}{\partial T}\right)_{EB}$, $\left(\frac{\partial T}{\partial B_\beta}\right)_{SE}$, $\left(\frac{\partial P_\alpha}{\partial B_\beta}\right)_{TE}$, which enter modified [16] Eq.(1) and Eq.(2).

The bulk sample of BiFeO₃ is simulated by a 12x12x12 supercell with periodic boundary conditions applied along all three directions. Every tenth simulation is cross checked by using 20x20x20 supercell. The total energy of this supercell is given by the effective Hamiltonian [17, 18] with the parameters derived from density functional theory calculations [19]. The degrees of freedom for the Hamiltonian include local mode that is proportional to the dipole moment in the unit cell, magnetic dipole moment and local strain variables. In this work the Hamiltonian is extended to incorporate the magnetic degrees of freedom similarly to the approach of Ref.20. More precisely, the total energy of the Hamiltonian includes the magnetic exchange interaction, the interaction between magnetic moments and elastic deformations, and the on-site interactions between magnetic moments and local modes. The latter one originates from the spin-orbit interaction and is quadratic in both local mode and magnetic moment. This Hamiltonian reproduces a variety of structural, thermodynamical and dynamical properties of BiFeO₃ which include the polarization, antiferromagnetic order

parameter, Curie and Néel temperatures [21], tetragonality, and some others. To compute the zero-field isothermal coupling $\left(\frac{\partial P_\alpha}{\partial B_\beta}\right)_{TE}$ we use linear response theory [22] in the framework of Metropolis Monte Carlo algorithm [23]. We find this coupling to be of the order of 10^{-7} which is smaller than the error bar of our computations. The only exceptions are the temperatures around the Curie point where we find $\left(\frac{\partial P_\alpha}{\partial B_\alpha}\right)_{TE}$ up to $5.3 \cdot 10^{-6} \pm 2.2 \cdot 10^{-6}$ relative to vacuum. This is in line with the current literature [7]. $\left(\frac{\partial A_\alpha}{\partial E_\beta}\right)_{TB}$ is taken to be equal to zero since we assume that the electric field does not couple to the antiferromagnetic vector directly.

Furthermore, the zero-field $\left(\frac{\partial P_\alpha}{\partial T}\right)_{EB}$ and $\left(\frac{\partial A_\alpha}{\partial T}\right)_{EB}$ are computed from the temperature evolution of polarization and antiferromagnetic vectors, respectively. They are reported in Fig.1(a) and (b). We notice that $\left|\left(\frac{\partial P_\alpha}{\partial T}\right)_{EB}\right|$ and $\left|\left(\frac{\partial A_\alpha}{\partial T}\right)_{EB}\right|$ are maximized near Curie and Néel temperatures, respectively. To obtain $\left(\frac{\partial T}{\partial E_\beta}\right)_{SB}$ and $\left(\frac{\partial T}{\partial B_\beta}\right)_{SE}$ we compute electrocaloric and magnetocaloric effects using isentropic Monte Carlo [15]. In such simulations the temperature is calculated during a slow adiabatic application of electric or magnetic field. Technically, the electric field is applied at an extremely low rate of 50 V/m per one Monte Carlo sweep to ensure reversibility. Similarly the rate of application for the magnetic induction is 0.5 mT per Monte Carlo sweep. The linear region in the field evolution of the temperature is used to compute the derivatives. They are given in Fig.1(c) and (d). Once again we find that these linear effects reach their extremums near Curie and Néel temperatures. Interestingly, the magnetocaloric effect (see Fig.1(c)) changes its sign from positive to negative in the vicinity of Néel temperature. The effect, however, is rather small due to very small magnetic susceptibility of antiferromagnetic BiFeO₃.

To compute the isentropic couplings $\left(\frac{\partial P_\alpha}{\partial B_\alpha}\right)_{SE}$ and $\left(\frac{\partial A_\alpha}{\partial E_\alpha}\right)_{SB}$ the derivatives shown in Fig.1 are used in modified Eq.(1) and Eq.(2) where we neglect the contribution from the isothermal couplings (the last term). The computational data for $\left(\frac{\partial P_\alpha}{\partial B_\alpha}\right)_{SE}$ and $\left(\frac{\partial A_\alpha}{\partial E_\alpha}\right)_{SB}$ are given in Fig.2 in dimensionless units. Note that in the figure we report the diagonal component of the magnetoelectric coupling tensor.

Fig.2 demonstrates that the isentropic couplings are nonzero even in materials with vanishing isothermal response. Fig.2(a) reports the computational data for the isentropic electromagnetic coupling. Generally, we do not expect this coupling to be large in BiFeO₃ owing to its antiferromagnetic nature and associated ultralow magnetocaloric effect. Nevertheless,

we find that the isentropic $\left(\frac{\partial P_\alpha}{\partial B_\beta}\right)_{SE}$ exceeds the isothermal $\left(\frac{\partial P_\alpha}{\partial B_\beta}\right)_{TE}$ by orders of magnitude. One can further dramatically enhance the isentropic coupling by heterostructuring BiFeO₃ with good magnetocaloric materials. If we consider a heterostructure of BiFeO₃ with one of the best magnetocaloric material - single crystal Gd [24] - we find that $\left(\frac{\partial P_\alpha}{\partial B_\beta}\right)_{SE}$ could be increased by three orders of magnitude! For instance, the adiabatic application of 2 T magnetic field to Gd single crystal at room temperature causes the temperature to increase by 6.3 K [24]. Eq.(2) predicts that the associated decrease in polarization can reach up to 1.85 mC/m². By further inspection of Fig.2(a) we note that in BiFeO₃ $\left(\frac{\partial P_\alpha}{\partial B_\beta}\right)_{SE}$ could be both positive and negative and reaches extreme values near the Curie and Néel temperatures. Interestingly, we also find that in BiFeO₃ $\left(\frac{\partial A_\alpha}{\partial E_\alpha}\right)_{EB}$ exceeds significantly $\left(\frac{\partial P_\alpha}{\partial B_\alpha}\right)_{SE}$.

We next verify the predictions obtained from Eqs.(1) and (2) in direct computations. Fig.2 indicates that the extremal response is expected around temperatures 880 K and 1200 K. To that end we compute the change in polarization and antiferromagnetic vector under slow adiabatic application of magnetic induction and electric field, respectively, around these temperatures. Fig.3 shows the dependence of the polarization on magnetic induction at $T = 840$ K (panel (a)), $T = 1000$ K (panel (b)) and the dependence of antiferromagnetic vector on the electric field at $T = 790$ K (panel (c)). Note, that due to relatively low ratio of magnetoelectric effect to thermal noise we choose to report the data for very high magnetic fields for the purpose of demonstration. Since Fig.3 shows that for the chosen temperatures the response of the polarization to the magnetic induction is linear the results are easily scaled down to fields of practical importance. The figure reveals the existence of isentropic electromagnetic coupling. The effect is in both qualitative and quantitative agreement with the predictions from Eqs.(1) and (2) given by the solid lines.

Our simulations demonstrate that in multiferroics the isentropic and isothermal electro-magnetic couplings can be orders of magnitude different. At the same time, in experiments the processes are typically neither completely isentropic (adiabatic) nor isothermal. As a result, depending on the experimental conditions the observed electromagnetic response is likely to have both isothermal and isentropic contributions. Time could be an important factor in determining these contributions. For example, in experiments that are carried out on a time scale shorter than the one required to reach thermal equilibrium with the environment the isentropic response is likely to dominate. Similarly, in experiments where adiabatic conditions are carefully maintained (as in the experiments on direct measurements of caloric

effects [25]) the isentropic response will prevail. On the opposite end, if experimental measurements are taken when the sample is in thermal equilibrium with the surroundings then the isothermal response can be isolated.

In summary, we proposed a way to enhance the magnetoelectric coupling in magnetoelectric multiferroics through temperature mediated mechanism. Such mechanism couples magnetization to the electric field (polarization to the magnetic induction) indirectly by taking advantage of pyromagnetic and electrocaloric (pyroelectric and magnetocaloric) properties of the material. This is especially attractive in the light of recent reports of giant caloric effects in ferroics [26–32]. Such an approach was tested in both direct and indirect first-principles-based simulations and revealed that a significant enhancement of magnetoelectric coupling could be achieved. The advantage of this unusual strategy is that it could be applied to both intrinsic and extrinsic multiferroics which is likely to open a variety of ways to engineer materials with desirable magnetoelectric response.

Financial support for this work provided by the National Science Foundation Grant, No DMR-1250492.

-
- [1] J. Wang, J. B. Neaton, H. Zheng, V. Nagarajan, S. B. Ogale, B. Liu, D. Viehland, V. Vaithyanathan, D. G. Schlom, U. V. Waghmare, N. A. Spaldin, K. M. Rabe, M. Wuttig, and R. Ramesh, *Science* **299**, 1719 (2003).
 - [2] T. Kimura, T. Goto, H. Shintani, K. Ishizaka, T. Arima, and Y. Tokura, *Nature* **426**, 55 (2003).
 - [3] Y.-H. Chu, L. W. Martin, M. B. Holcomb, M. Gajek, S.-J. Han, Q. He, N. Balke, C.-H. Yang, D. Lee, W. Hu, Q. Zhan, P.-L. Yang, A. Fraile-Rodriguez, A. Scholl, S. X. Wang, and R. Ramesh, *Nat. Mater.* **7**, 478 (2008).
 - [4] H. Jang, S. Baek, D. Ortiz, C. Folkman, R. Das, Y. Chu, P. Shafer, J. Zhang, S. Choudhury, V. Vaithyanathan, Y. Chen, D. Felker, M. Biegalski, M. Rzchowski, X. Pan, D. Schlom, L. Chen, R. Ramesh, and C. Eom, *Phys. Rev. Lett.* **101**, 107602 (2008).
 - [5] B. Lorenz, A. Litvinchuk, M. Gospodinov, and C. Chu, *Phys. Rev. Lett.* **92**, 087204 (2004).
 - [6] S. Park, Y. Choi, C. Zhang, and S.-W. Cheong, *Phys. Rev. Lett.* **98**, 057601 (2007).
 - [7] K. Wang, J.-M. Liu, and Z. Ren, *Adv. Phys.* **58**, 321 (2009).

- [8] M. Bibes and A. Barthelémy, Nat. Mater. **7**, 425 (2008).
- [9] W. Eerenstein, N. D. Mathur, and J. F. Scott, Nature **442**, 759 (2006).
- [10] R. Ramesh and N. A. Spaldin, Nat. Mater. **6**, 21 (2007).
- [11] N. A. Hill, J. Phys. Chem. B **104**, 6694 (2000).
- [12] A. Van Run, D. Terrell, and J. Scholing, J. Mater. Sci. **9**, 1710 (1974).
- [13] C.-W. Nan, M. Bichurin, S. Dong, D. Viehland, and G. Srinivasan, J. Appl. Phys. **103**, 031101 (2008).
- [14] R. E. Newnham, *Properties of Materials* (Oxford, 2005).
- [15] I. Ponomareva and S. Lisenkov, Phys. Rev. Lett. **108**, 167604 (2012).
- [16] The modification is to replace M with A .
- [17] W. Zhong, D. Vanderbilt, and K. M. Rabe, Phys. Rev. Lett. **73**, 1861 (1994).
- [18] W. Zhong, D. Vanderbilt, and K. Rabe, Phys. Rev. B **52**, 6301 (1995).
- [19] C.-M. Chang, B. K. Mani, S. Lisenkov, and I. Ponomareva, “Prediction of electromagnons in antiferromagnetic ferroelectrics from first-principles: The case of BiFeO_3 ,” To be published.
- [20] I. A. Kornev, S. Lisenkov, R. Haumont, B. Dkhil, and L. Bellaiche, Phys. Rev. Lett. **99**, 227602 (2007).
- [21] Note that the Hamiltonian overestimates the Néel temperatures of BiFeO_3 which is attributed to the well known difficulties of density functional theory in predicting magnetic states in BiFeO_3 [?].
- [22] D. Frenkel and B. Smit, *Understanding Molecular Simulations: from Algorithms to Applications* (Academic Press, 2002).
- [23] N. Metropolis, A. W. Rosenbluth, M. N. Rosenbluth, A. H. Teller, and E. Teller, J. Chem. Phys. **21**, 1087 (1953).
- [24] K. A. Gschneidner and V. K. Pecharsky, Annu. Rev. Mater. Sci. **30**, 387 (2000).
- [25] Y. Bai, G. Zheng, and S. Shi, Appl. Phys. Lett. **96**, 192902 (2010).
- [26] V. K. Pecharsky and K. A. Gschneidner, Jr., Phys. Rev. Lett. **78**, 4494 (1997).
- [27] O. Tegus, E. Bruck, K. H. J. Buschow, and F. R. de Boer, Nature **415**, 150 (2002).
- [28] A. S. Mischenko, Q. Zhang, J. F. Scott, R. W. Whatmore, and N. D. Mathur, Science **311**, 1270 (2006).
- [29] E. Bonnot, R. Romero, L. Mañosa, E. Vives, and A. Planes, Phys. Rev. Lett. **100**, 125901 (2008).

- [30] B. Neese, B. Chu, S.-G. Lu, Y. Wang, E. Furman, and Q. Zhang, *Science* **321**, 821 (2008).
- [31] L. Manosa, D. Gonzalez-Alonso, A. Planes, E. Bonnot, M. Barrio, J.-L. Tamarit, S. Aksoy, and M. Acet, *Nat. Mater.* **9**, 478 (2010).
- [32] L. Manosa, D. Gonzalez-Alonso, A. Planes, M. Barrio, J.-L. Tamarit, I. S. Titov, M. Acet, A. Bhattacharyya, and S. Majumdar, *Nat. Commun.* **2**, 595 (2011).

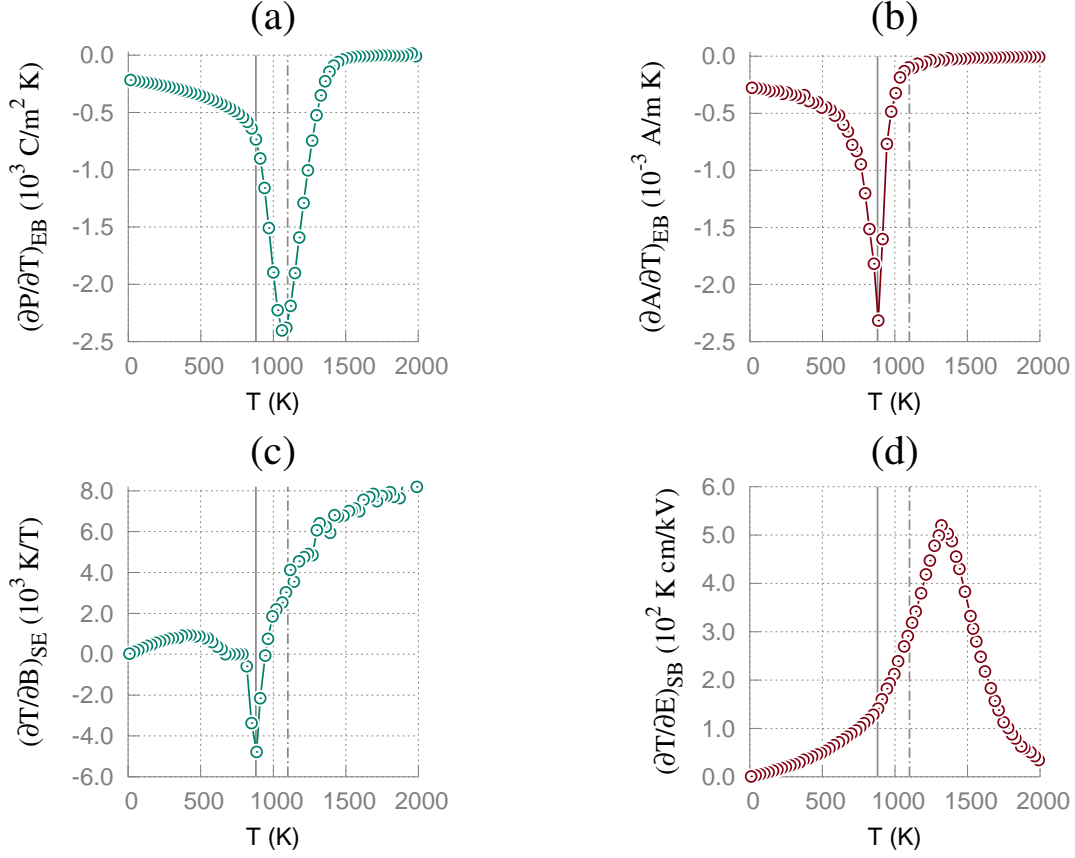


FIG. 1. Temperature dependence of the pyroelectric coefficient (a); the coupling coefficient between the antiferromagnetic order parameter and temperature (b); linear magnetocaloric effect (c); and linear electrocaloric effect (d). Solid and dot-dashed vertical lines give computational Néel and Curie temperature, respectively.

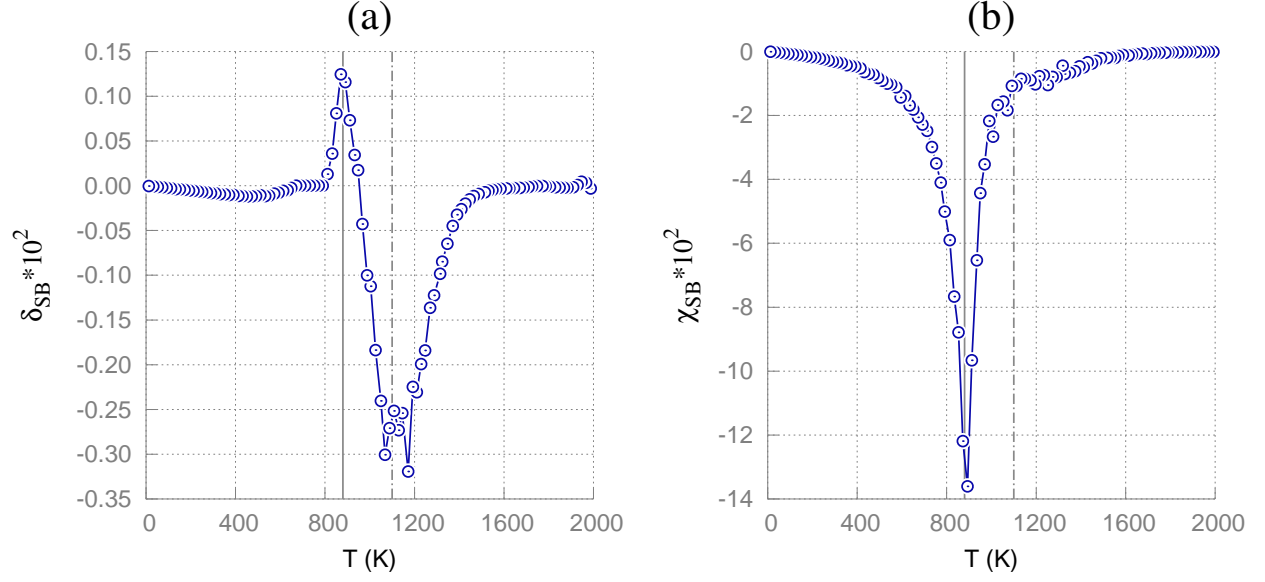


FIG. 2. Temperature dependence of the isentropic electromagnetic coefficient $\delta_{SB} = \left(\frac{\partial P_\alpha}{\partial B_\alpha} \right)_{SE} \sqrt{\frac{\mu_0}{\varepsilon_0}}$ in units relative to vacuum (a); and “antiferromagnetoelectric” response $\chi_{SB} = \left(\frac{\partial M_\alpha}{\partial E_\alpha} \right)_{SB} \sqrt{\frac{\mu_0}{\varepsilon_0}}$ in units relative to vacuum (b).

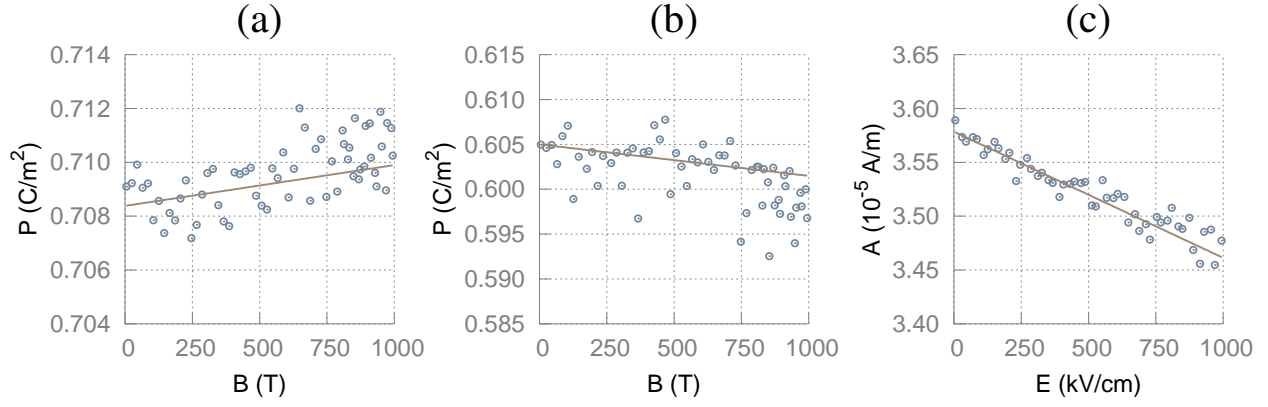


FIG. 3. Dependence of the polarization on magnetic field applied isentropically at $T = 840$ K (panel (a)) and $T = 1000$ K (panel (b)). Panel (c) gives the dependence of antiferromagnetic vector on electric field applied isentropically at $T = 790$ K. Solid lines give predictions from thermodynamic Eq.(2) and modified Eq.(1).